A multi-model framework to estimate perfusion parameters using contrast-enhanced ultrasound imaging

Alireza Akhbardeh
Department of Radiology, Stanford University School of Medicine, Stanford, CA 94305, USA

Hersh Sagreiya
Department of Radiology, Stanford University School of Medicine, Stanford, CA 94305, USA
Department of Biomedical Data Science, Stanford University, Stanford, CA 94305, USA

Ahmed El Kaffas, and Jürgen K. Willmann*
Department of Radiology, Stanford University School of Medicine, Stanford, CA 94305, USA

Daniel L. Rubin[a)]
Department of Radiology, Stanford University School of Medicine, Stanford, CA 94305, USA
Department of Biomedical Data Science, Stanford University, Stanford, CA 94305, USA
Department of Medicine (Biomedical Informatics Research), Stanford University, Stanford, CA 94305, USA

(Received 23 May 2018; revised 3 October 2018; accepted for publication 7 November 2018; published 21 January 2019)

Purpose: Contrast-enhanced ultrasound imaging has expanded the diagnostic potential of ultrasound by enabling real-time imaging and quantification of tissue perfusion. Several perfusion models and curve fitting methods have been developed to quantify the temporal behavior of tracer signal and standardize perfusion quantification. While the least-squares approach has traditionally been applied for curve fitting, it can be inadequate for noisy and complex data. Moreover, previous research suggests that certain perfusion models may be more relevant depending on the organ or tissue imaged. We propose a multi-model framework to select the most appropriate perfusion model and curve fitting method for each diagnostic application.

Methods: Our multi-model approach uses a system identification method, which estimates perfusion parameters from the model with the best fit to a given time–intensity curve. We compared current perfusion quantification methods that use a single perfusion model and curve fitting method and our proposed multi-model framework on bolus 3D dynamic contrast-enhanced ultrasound (DCE-US) *in vivo* images obtained in mice implanted with a colon cancer, as well as on simulation data. The quality of fit in estimating perfusion parameters was evaluated using the Spearman correlation coefficient, the coefficient of determination (R^2), and the normalized root-mean-square error (NRMSE) to ensure that the multi-model framework finds the best perfusion model and curve fitting algorithm.

Results: Our multi-model framework outperforms conventional single perfusion model approaches with least-squares optimization, providing more robust perfusion parameter estimation. R^2 and NRMSE are 0.98 and 0.18, respectively, for our proposed method. By comparison, the performance of the traditional approach is much more dependent upon the selection of the appropriate model. The R^2 and NRMSE are 0.91 and 0.31, respectively.

Conclusions: The proposed multi-model framework for perfusion modeling outperforms the current approach of single perfusion modeling using least-squares optimization and more robustly estimates perfusion parameters when using empiric data labeled by an expert as the gold standard. Our technique is minimally sensitive to issues affecting the accuracy of perfusion parameter estimation, including rise time, noise, region of interest size, and frame rate. This framework could be of key utility in modeling different perfusion systems in different tissues and organs. © *2018 American Association of Physicists in Medicine* [https://doi.org/10.1002/mp.13340]

Key words: contrast-enhanced ultrasound, curve fitting, perfusion modeling, system identification

1. INTRODUCTION

Contrast-enhanced ultrasound (CEUS) is increasingly utilized as a diagnostic tool due to its increased commercial and clinical availability, both in the United States and globally.[1–3] Microbubbles, consisting of a gas core stabilized by a shell composed of protein, lipids, or polymers, serve as the indicator tracer in CEUS, and microbubble signal can be isolated from the surrounding tissue signal using microbubble-specific imaging techniques,[1] by which the acoustic intensity of microbubbles is proportional to the concentration of microbubbles in a given region of interest (ROI).[4,5] Several methods exist for contrast administration and acquisition, and multiple protocols have been developed to improve qualitative and quantitative assessments.[2,3] Measurements from 3D dynamic CEUS have been shown to be repeatable in

patients.[6] Bolus-based imaging remains the dominant CEUS method,[5,7,8] and it is commonly utilized as a qualitative method for arriving at a differential diagnosis. Moreover, several new quantitative CEUS applications are on the horizon. These applications include, but are not limited to, treatment monitoring, cardiology, neuroimaging, musculoskeletal imaging, and abdominal imaging.[5,7,8] Cancer treatment monitoring is of particular interest given the plethora of vascular-targeting cancer drugs in recent years. These often induce cytostatic responses (i.e., no change in tumor size with change in perfusion), with minimal anatomical changes over time.[1–3] Since the tumor will not have changed in size, traditional ultrasound measurements will fail to notice any change, while quantitative measures of perfusion using CEUS will.[9,10] While the current treatment response evaluation of cancer is performed using CT and MRI, CEUS has the ability to contribute real-time data on tumor perfusion, an advantage over contrast-enhanced CT and MRI. Thus, as quantitative analysis becomes more commonly used in the clinic, new and improved quantification methods are needed.

Perfusion data from CEUS are conventionally quantified by fitting an established perfusion model to a time–intensity curve (TIC) extracted from a ROI, from which several parameters related to blood flow and volume are extracted. These parameters include area under the time–intensity curve (AUC) and peak enhancement (PE), which are related to blood volume, as well as mean transit time (MTT) and time to the peak intensity (TP), which are related to blood flow. Curve fitting is typically performed using least-squares optimization, which is inadequate in the setting of noisy or complex data. Time–intensity curves are susceptible to the following issues: (a) data quality (affected by noise and ROI size), (b) frame rate, and (c) rise time. In the Results section, we demonstrate how these conditions can affect the quality of the fit to TICs and thus the estimation of perfusion parameters. In addition, given the numerous applications for CEUS in different organs or tissues, it is imperative to select the appropriate model for a given application. We propose a multi-model framework that can automatically select the correct model, which works well both on real and simulated data.

Our study briefly reviews the following perfusion models: lognormal, gamma variate, local density random walk (LDRW), first passage time (FPT), and lagged normal. Lognormal is the most commonly used perfusion model.[11,12] We then develop a multi-model system identification[13] approach for automated model selection based on best fit, and we evaluate the performance of this approach against the conventional single perfusion model with least-squares optimization. Least-squares optimization is the most commonly used curve fitting method. System identification is an engineering field that involves identifying the dynamics between the inputs and outputs of a model. We selected the optimal curve fitting algorithm and perfusion model using an exhaustive search technique.[14] Exhaustive search performs well in a multivariate situation, in which there is no definite single solution, by testing each possibility sequentially and determining whether it satisfies the problem statement or cost function. We then test our multi-model approach in simulations. Finally, we apply our approach to *in vivo* DCE-US images from a mouse model of colon cancer.

2. BACKGROUND/THEORY

2.A. Multi-model framework

The single perfusion model currently used to estimate perfusion parameters is very sensitive to the initial values for perfusion parameters, as well as the selection of appropriate boundary conditions, without which the algorithm could result in unrealistic values for perfusion parameters, such as a negative value for time to peak. We introduce a multi-model framework, which applies two different curve fitting algorithms (nonlinear regression (NR) and a mixed-effects (ME) method) to all five perfusion models (lognormal, gamma variate, LDRW, FPT, and lagged normal). All curve fitting algorithms and perfusion models are detailed in the next section. We propose using more than one curve fitting algorithm because if the initial values and boundary conditions are not manually set to the proper values, then the fitting performance for different perfusion models can be inconsistent, potentially settling on local minima for which additional optimization to find the global minimum is required. Therefore, fusing the result of multiple perfusion models and curve fitting methods is a better approach to overcome poor boundary conditions. As shown in Fig. 1, all five perfusion models (lognormal, gamma variate, LDRW, FPT, and lagged normal) using the two curve fitting methods (NR and ME) were independently computed, and the final perfusion parameters were chosen from the model with the lowest estimation error by evaluating various curve fitting algorithms and selecting the optimal solution using an exhaustive search technique.[14] Since multiple measures of curve fitting were evaluated, Spearman correlation coefficient, coefficient of determination, and normalized root-mean-square error (NRMSE), this was done in a sequential fashion. Beginning with the initial ten techniques (five perfusion models with two curve fitting methods each), the Spearman correlation coefficient was used to select the five techniques with highest correlation. Next, among those five, the coefficient of determination was used to select the three techniques with the highest R^2. Finally, the one technique with the lowest NRMSE was chosen from those three. We use three cost functions rather than one because we want to overcome the issue of local minima in optimization, in which curve fitting may be trapped in parasitic stationary points that are not informative about the true parameters.[15] It has been suggested that the mean squared error is not necessarily the best criterion for model evaluation.[16] For instance, Harabis et al. (2013) compared different models for DCE-US perfusion analysis

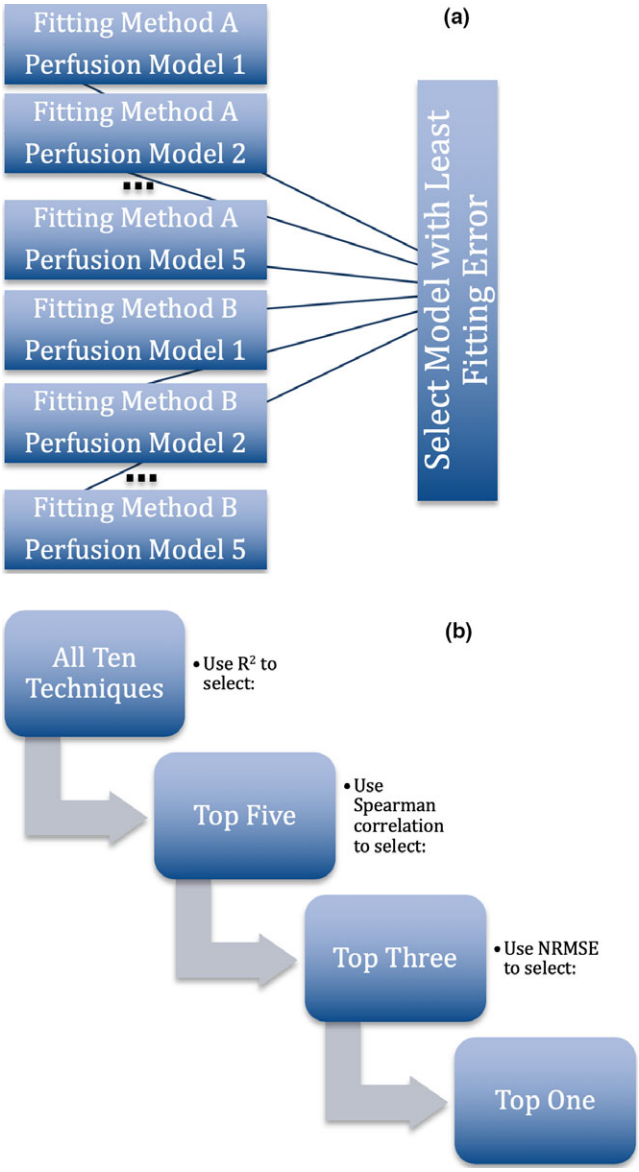

FIG. 1. The multi-model framework takes the input time–intensity curve and estimates perfusion parameters (t_0, area under the curve, time to peak, mean transit time, and peak enhancement). (a) Our proposed framework evaluates five perfusion models (lognormal, gamma variate, local density random walk, first passage time, and lagged normal) and two curve fitting methods (nonlinear regression and mixed-effects). (b) To determine the parameters obtained using the optimal curve fitting method/perfusion model, we start with the ten techniques from (a), and the model with the least fitting error was chosen as follows: 1) The Spearman correlation coefficient was used to select the five techniques with the highest correlation value, 2) The coefficient of determination was then used to select the three techniques with the highest R^2, and 3) the one technique with the lowest normalized root-mean-square error was finally chosen. This technique is known as exhaustive search. [Color figure can be viewed at wileyonlinelibrary.com]

and concluded that more models should be used, specifically excluding the lognormal model, which gives the highest error, particularly for the MTT parameter. In order to mitigate the local minima problem, many alternatives to the standard least-squares problem have been proposed,[17,18] extending the parameter space to multiple cost functions. To overcome issues with the least-squares method mainly due to local minima in the optimization process, which is of particular concern with noisy data, we proposed using a three-step approach.

2.B. Perfusion models

We studied five different perfusion models commonly used in clinical CEUS: the lognormal distribution, the gamma variate function, LDRW, FPT, and the lagged normal function. Each model is best suited to different tissues (i.e., liver vs heart). Generally, these models are described by a probability density function of pixel intensities over time within a VOI after a bolus of microbubbles is injected. Table I shows the distribution function for each model, as well as the organ system for which it has been considered a good fit by the literature.[19]

2.B.1. Lognormal model

This model is based on the bifurcations of vessels with a number of generations, which may exhibit fractal behavior.[20,21] The control parameters for the lognormal distribution are AUC, t_0, C, μ, and σ, representing the area under the curve, offset time, baseline intensity offset, mean, and standard deviation, respectively, of the normal distribution in logarithmic space. A similar notation is used for the corresponding parameters in all subsequent models discussed. The distribution function is shown in the second column of Table I and an example curve is shown in the third column of Table I for AUC = 30, t_0 = 10, C = 0, μ = 3, and σ = 1.

2.B.2. Gamma variate model

This model is based on constant flow through a series of equally sized and homogeneous compartments.[22] The distribution function is shown in Table I, column 2. The control parameters for this model include AUC, t_0, C, α, and β, respectively representing the area under the curve, the offset time, the baseline intensity offset, the number of the equally sized homogeneous compartments in a series, and the volume of each compartment divided by the flow rate. An example curve is shown in the third column of Table I for AUC = 30, t_0 = 10, C = 0, α = 3, and β = 6.

2.B.3. Local density random walk model

This distribution is designed to model fluid convection and diffusion within a tube (or vessel in our case).[23,24] The distribution function is shown in Table I, column 2. The control parameters for this model are AUC, t_0, C, μ, and λ, respectively representing the area under the curve, offset time, baseline intensity offset, mean, and the Preclet number divided by 2. For a vessel in which a bolus of microbubbles is flowing, the Preclet number is defined as

TABLE I. Definition and application of perfusion models.

	Distribution function		Perfusion Parameters	Best fit to
Lognormal	$I(t)=\frac{\text{AUC}}{\sqrt{2\pi}\sigma(t-t_0)}e^{\frac{[\ln(t-t_0)-\mu]^2}{2\sigma^2}}+C$	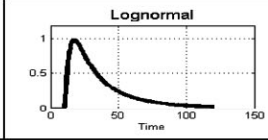	$\text{MTT}=e^{\mu+\sigma^2/2},$ $t_p=e^{\mu-\sigma^2}$	Breast, Heart
Gamma Variate	$I(t)=\frac{\text{AUC}}{\beta^{\alpha+1}\Gamma(\alpha+1)}(t-t_0)^{\alpha}e^{-\frac{(t-t_0)}{\beta}}+C$	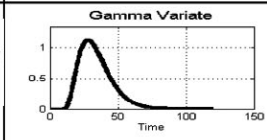	$\text{MTT}=\beta(\alpha+1)$ $t_{\text{p}}=\alpha\cdot\beta.$	Carotid
LDRW	$I(t)=\text{AUC}\cdot\left(\frac{e^{\lambda}}{\mu}\right)\sqrt{\frac{\mu}{(t-t_0)}\frac{\lambda}{2\pi}}$ $\cdot\exp\left[-\frac{1}{2}\lambda\left(\frac{\mu}{(t-t_0)}+\frac{(t-t_0)}{\mu}\right)\right]+C$	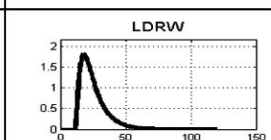	$\text{MTT}=\mu$ $t_{\text{p}}=\left(\frac{\mu}{2\lambda}\right)(\sqrt{1+4\lambda^2}-1)$	Carotid
FPT	$I(t)=\text{AUC}\cdot\left(\frac{e^{\lambda}}{\mu}\right)\cdot\sqrt{\frac{\lambda}{2\pi}}\cdot\left(\frac{\mu}{(t-t_0)}\right)^{3/2}$ $\cdot\exp\left[-\frac{1}{2}\lambda\left(\frac{\mu}{(t-t_0)}+\frac{(t-t_0)}{\mu}\right)\right]+C$	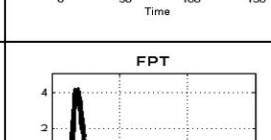	$\text{MTT}=\mu$ $t_{\text{p}}=\frac{\mu}{2\lambda}(\sqrt{9+4\lambda^2}-3)$	Carotid
Lagged Normal	$I(t)=\frac{\text{AUC}}{2}\lambda\exp\left\{-\lambda(t-t_0)-\frac{\mu^2}{2\sigma^2}+\frac{(\mu+\lambda\sigma^2)^2}{2\sigma^2}\right\}$ $\left[1+erf\left(\frac{(t-t_0)-\mu-\lambda\sigma^2}{\sqrt{2\sigma^2}}\right)\right]+C$	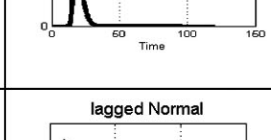	$\text{MTT}=\mu+\frac{1}{\lambda}$	Liver

The mean transit time (MTT) and the time to peak intensity (t_P) for each model are shown in the fourth column.

the ratio between the diffusive time and the convective time, estimating the contribution of both the diffusion and the convection of the microbubbles traveling through the vessels. An example curve is shown in the third column of Table I for AUC = 30, t_0 = 10, C = 0, μ = 10, and λ = 2.

2.B.4. First passage time model

Similar to LDRW, this distribution is designed to model fluid convection and diffusion within a tube (i.e., vessel). The only difference between FPT and LDRW is that in FPT the microbubbles are assumed to pass only once through the vessel boundaries, whereas the LDRW model assumes that microbubbles pass the boundaries multiple times.[23,24] The distribution function is shown in Table I, column 2. The control parameters for this model are AUC, t_0, C, μ, and λ, where they respectively represent the area under the curve, offset time, baseline intensity offset, mean, and the Preclet number divided by 2. An example curve is shown in the third column of Table I for AUC = 30, t_0 = 10, C = 0, μ = 10, and λ = 10.

2.B.5. Lagged normal model

This distribution is designed for scenarios in which the dispersion of microbubbles in large vessels is random with a normal or Gaussian distribution followed by exponential merging through a micro-vascular network.[25] The distribution function is shown in Table I, column 2. The control parameters for this model are AUC, t_0, C, μ, σ, and λ, where they respectively represent the area under the curve, offset time, baseline intensity offset, mean, standard deviation, and the Preclet number divided by 2. An example curve is shown in the third column of Table I for AUC = 30, t_0 = 10, C = 0, μ = 10, and λ = 2.

2.C. Curve fitting methods

Curve fitting is used to fit a given perfusion model to TIC data. Curve fitting requires a parametric model (perfusion model) that connects the response data to the observed data by using optimization techniques to solve the model and estimate model coefficients. The most commonly used optimization method to obtain model coefficients is least-squares

optimization, which minimizes the sum of the squared error (residual) between each observed response and estimated response. To minimize the influence of outliers, a major drawback of least-squares fitting, the more robust least-squares regression has been developed, which minimizes a weighted sum of squares in which the weight for each data point is based on the distance between that point and the fitted point. Points that are near the fitted point get full weight, whereas points further from the fitted point have less weight.[26,27] We applied an alternative approach for curve fitting described below:

2.C.1. Mixed-effect models

Data from the TICs were input into a ME model for curve-fitting.[28] For additional details regarding mixed-effects models, please see the Appendix S1.

2.C.2. Nonlinear regression based models

Data from the TICs were input into NR models for curve fitting.[29,30] For additional details regarding nonlinear regression based models, please see the Appendix S1.

2.D. Factors affecting curve fitting

1) An incorrect offset time can lead to failure in perfusion parameter estimation. Boundary conditions and the initial values for the perfusion parameters, particularly the offset time, play a key role in the current method of least-squares optimization. If the user-chosen boundary conditions are not close to the expected values, the least-squares method will likely fail. Therefore, the user will need to try several boundary conditions to determine which one works,[31] which is impractical when studying multiple tumors, particularly when the goal is the automation of imaging analysis.

2) Data quality also critically affects perfusion parameter estimation. If the TIC data are very noisy with frequent spikes and outliers, perfusion parameter estimation can fail. In particular, if the ROI size is small, the resulting TIC data will be substantially noisier. Since the number of pixels used to calculate TIC values by averaging pixel intensities will be fewer with a smaller ROI, the outcome will naturally be a nosier TIC.

3) Frame rate, or temporal resolution, could also affect the estimation of perfusion parameters, as sampling a smaller number of data points in a given time period could potentially affect the performance of curve fitting algorithms.

3. MATERIALS AND METHODS

3.A. Imaging technique

The data analysis for the 3D dynamic contrast-enhanced (DCE) imaging datasets was performed using custom software developed in Matlab R2015b (MathWorks, Natick, MA, USA). The data analysis pipeline includes three major steps:

1) Pre-processing (image analysis): the input image dataset consists of 3D contrast-mode imaging data spanning all of the time points acquired during the course of contrast ultrasound imaging. Ultrasound voxel values in contrast-mode images were linearized with a transformation function and a compression parameter provided by the equipment manufacturer, as previously described.[6,32] If needed, 3D re-slicing (re-sampling) is applied to convert the number of 3D slices and the image matrix size to the target matrix size.

2) Extracting TICs: linearized voxel intensities within a user-defined volume of interest (VOI) are used to obtain TICs. The time–intensity values within the VOI at each time point are plotted to generate a TIC, with intensity related to microbubble concentration. We developed a toolset in Matlab that allows the user to manually contour a free-shape VOI in order to cover the entire tumor visualized in the sagittal, longitudinal, and coronal planes.

3) Computing perfusion parameters: a first-pass kinetic analysis of the TIC from the VOI, based on the wash-in and wash-out kinetics of the microbubbles after bolus injection, is used to quantify tumor perfusion. Perfusion parameters of the tumor, including peak enhancement (PE, arbitrary units, au), area under the curve (AUC, au), mean transit time (MTT, seconds), and time to peak (TP, seconds), are calculated from the fitted TICs using different perfusion models: lognormal, gamma variate, LDRW, FPT, and lagged normal. AUC was defined as the area under the TIC. PE was defined as the maximum increase in the signal intensity following bolus injection of the contrast agent. TP was defined as the time interval until the peak of the fitted curve. MTT was provided from the various perfusion models. PE and AUC are related to blood volume, whereas TP and MTT are related to blood flow. Curve fitting to calculate perfusion parameters (PE, MTT, AUC, t_p) was performed using the traditional approach (nonlinear least-squares optimization) and our proposed multi-model framework, subsequently described.

3.B. Animal data acquisition

Data from ten mice imaged using three-dimensional CEUS were used for this study.[9] For additional details, please see the Appendix S2.

3.B.1. Evaluation of simulated data

In order to evaluate our proposed method for perfusion modeling against the current approach, we analyzed its performance using both simulated and real data. The proposed approach employed the aforementioned multi-model framework, which evaluates all five perfusion models. The current approach (least-squares optimization using the lognormal model) uses the least-squares cost function and the "Levenberg–Marquardt" or "Trust-Region" to fit a lognormal curve

to TIC data by varying fitting parameters (AUC, μ, σ, and t_0) and predicting the best parameters that provide the least error.[33] For simulated data, the "ground truth" was obtained based on the parameters of the original lognormal model, generating a "noise-free" TIC with fitting parameters of AUC, μ, σ, and t_0 and expected perfusion parameters of AUC, MTT, and t_p. In particular, we used AUC = 0.015, μ = 4.5, σ = 1.1, and t_0 = 30 to create the "noise-free" TIC. We compared how well both the traditional approach (least-squares optimization) and our proposed approach for perfusion parameter estimation (multi-model framework) compared to the ground truth data from this noise-free TIC. We did this by calculating the Spearman correlation coefficient and the NRMSE between the traditional or proposed approach and the ground truth. Although multiple types of noise exist, we specifically investigated the effect of adding Poisson noise.[34] Hence, we constructed a "noisy" TIC by adding a Poisson distribution of noise to reduce the signal-to-noise ratio and once again compared the performance of the traditional and proposed approaches for perfusion parameter estimation to this new ground truth data from the noisy TIC, again using the Spearman correlation coefficient and the NRMSE. A "noisy" TIC was reconstructed by adding a Poisson distribution with $\lambda = 2$, which reduces the signal-to-noise ratio to 18 dB. Signal-to-noise ratio was calculated using the built-in Matlab function, signal-to-noise ratio (*SNR*). Finally, the robustness of the traditional and proposed methods to increasing levels of noise was determined by comparing estimated perfusion parameters to the ground truth values. Different levels of Poisson noise were added to reduce SNR (from 33 to 22, 18, 14, and 13) and investigate the effect of increasing noise on estimated parameters.

3.B.2. Evaluation of animal data

The impact of common factors affecting the quality of fit to animal data was studied. These include offset time (t_0), data quality (noise, ROI size), and frame rate. TIC data came from DCE-US of a typical mouse tumor. In order to establish the ground truth for this real data,[35] we wrote a script for the initial calculation of AUC, PE, and time to peak (TTP), and then by visual inspection we evaluated the veracity of the code suggestion (essentially representing a semi-manual method for deriving these values). While AUC could be defined as the sum at each time point and PE and TTP could be defined using the maximal value of the TIC data, MTT cannot be empirically derived. Next, a comparative analysis of the individual perfusion models was performed, with the raw TIC data from DCE-US of a typical mouse tumor once again serving as the ground truth. Finally, a cross-subject statistical analysis was performed, comparing the robustness of both the traditional approach and the proposed approach on TIC data from ten mouse cases. Once again, the ground truth perfusion parameters were empirically calculated. Finally, across three measures of goodness-of-fit (R^2, NRMSE, Spearman correlation coefficient), the mean, median, and standard deviation were calculated for the data from ten mice.

4. RESULTS

4.A. Simulated data

We compared the performance of both our proposed approach and the current approach for perfusion modeling (a single perfusion model, the lognormal distribution function, with the least-squares curve fitting method) using simulated data (Fig. 2) employing either a noise-free or noisy TIC. As can be seen, the proposed method outperforms the existing method, both using the "noise-free" TIC [Fig. 2(a)] and the "noisy TIC" [Fig. 2(b)]. As is evident in the figure, the current approach resulted in a value for t_0 that was off. Moreover, as increasing noise is applied to progressively degrade the signal-to-noise ratio [Fig. 2(c)], the proposed method is much more robust to dramatic increases in noise compared to the current method, deviating much less from the ground truth.

4.B. Animal data

We also compared the performance of the proposed approach and the current approach for perfusion modeling (single perfusion model with the least-squares curve fitting method) using mouse experimental data.

4.C. Performance evaluation

4.C.1. Offset time effect

We studied the impact of using different starting frames (and hence offset times) on curve fitting. Figure 3(a) shows the performance of the current method (least-squares) and our proposed technique for estimating perfusion parameters using a lognormal tracer model. As can be seen, if the offset time is large, then the existing technique might result in a poorer quality of fit if incorrect boundary conditions were initially set.

4.C.2. Data quality/noise effect

Figure 3(b) shows the performance of the current technique and our proposed technique to estimate perfusion parameters using the lognormal tracer model when the TIC data are noisy. As can be seen, the existing technique returns more deviated values for the perfusion parameters with noisy TIC data, while the estimations by the proposed technique are closer to the manually labeled ground truth.

4.C.3. Frame rate effect

Figure 3(c) and 3(d) simulate the effect of frame rate on curve fitting performance using both the current and proposed approaches with the lognormal tracer model. The simulation is performed by down-sampling the TIC data with

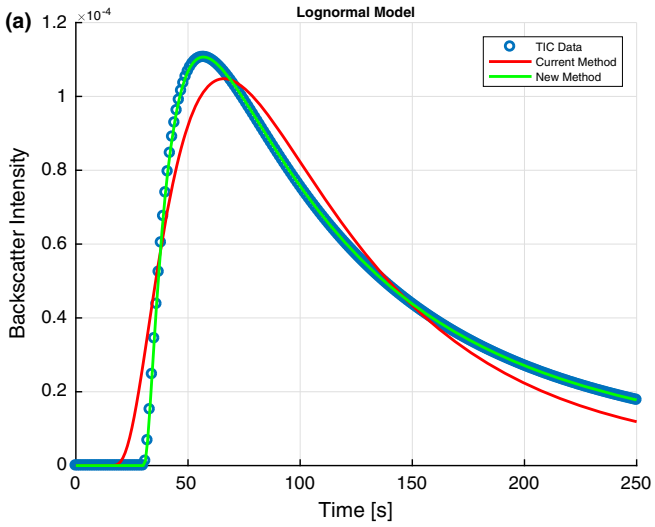

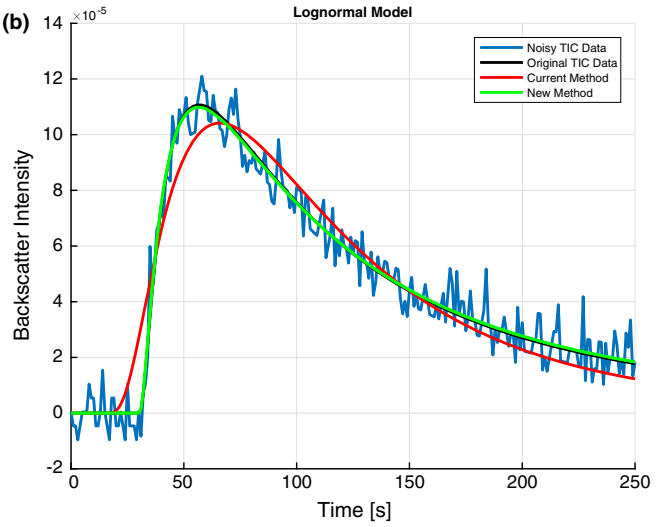

	Current Approach	New Approach
Correlation	97.64%	100%
NRMSE	0.21	0

	Ground Truth	Current Approach	New Approach
AUC	0.015	0.0128	0.015
t0	30	14.23	30
mtt	164.84	114.29	164.84
tp	26.84	51.70	26.84

	Current Approach	New Approach
Correlation	97.85%	99.99%
NRMSE	0.21	0.02

	Ground Truth	Current Approach	New Approach
AUC	0.015	0.0129	0.015
t0	30	14.71	30
mtt	164.84	115.82	172.9
tp	26.84	51.31	26.60

(c) **Proposed Method**

	Ground Truth	SNR=33	SNR=22	SNR=18	SNR=14	SNR=13	Average	Standard Deviation
AUC	0.015	0.015	0.015	0.015	0.015	0.015	0.015	0.00000
t_0	30	30	30.2	30.46	29.03	29.98	29.934	0.54109
MTT	164.84	164.16	166.81	175.42	164.46	183.88	170.946	8.55175
T_p	26.84	26.97	26.31	26.42	27.87	26.64	26.842	0.62751

Current Method

	Ground Truth	SNR=33	SNR=22	SNR=18	SNR=14	SNR=13	Average	Standard Deviation
AUC	0.015	0.0128	0.0128	0.0129	0.0133	0.0132	0.013	0.00023
t_0	30	14.184	13.96	14.257	14.753	15.44	14.5188	0.59084
MTT	164.84	114.32	113.1	116.6	116.25	120.08	116.07	2.65880
T_p	26.84	51.807	52.2	52.17	50.92	50.5	51.5194	0.76936

FIG. 2. Quality of fit for the current approach and our proposed approach for simulated data using the lognormal model as ground truth. (a) Results for a noise-free time–intensity curve: the Spearman correlation coefficient is higher with the new approach compared to the current approach, the normalized root-mean-squared error (NRMSE) is lower, and perfusion parameters (area under the curve, t_0, mean transit time, time to peak) are closer to the ground truth. (b) Results after adding Poisson noise: once again, the new method has a higher Spearman correlation coefficient, lower NRMSE, and perfusion parameters closer to the ground truth. (c) Ground truth vs estimated perfusion parameters with different levels of noise decreasing the SNR. As increased noise degrades the SNR, the individual perfusion parameters deviate much more from the ground truth with the current method compared to our new method. [Color figure can be viewed at wileyonlinelibrary.com]

different down-sampling factors. At any given down-sampling factor, our proposed approach clearly outperforms the current approach and only just begins to deviate from the expected result at a very high down-sampling factor of 16.

4.C.4. Comparative analysis of different perfusion models

We compared the performance of different perfusion models using the current (least-squares) and new techniques (multi-model framework). As can be seen in Fig. 4, which shows the raw mouse TIC data with circles, the existing technique for perfusion modeling is less accurate in estimating perfusion parameters, particularly for the LDRW and FPT tracer models. Several initial values and boundary conditions had to be manually set to find the best fit, requiring more than ten attempts to get right. As can be seen in the figure, the various perfusion models perform differently on the same TIC. As is evident in Fig. 4(c), if we use R^2 followed by Spearman correlation with the new method, the final model selection is the same as if we use Spearman correlation followed by R^2. Moreover, if we use NRMSE first followed by the other two, the results are still the same. In all cases, the final selection is LDRW.

4.C.5. Cross-subject Analysis

To investigate the performance and robustness of the proposed technique for perfusion modeling, we applied it to several mouse cases. Figure 5 compares perfusion parameters derived from the current approach and the proposed approach with empirical data. The figure shows that the proposed approach results in perfusion parameter estimation far closer to the empirical data. The data in Table II correspond with that in Fig. 5. The new method on average has a higher coefficient of determination, higher Spearman correlation coefficient, and lower normalized root-mean-square error.

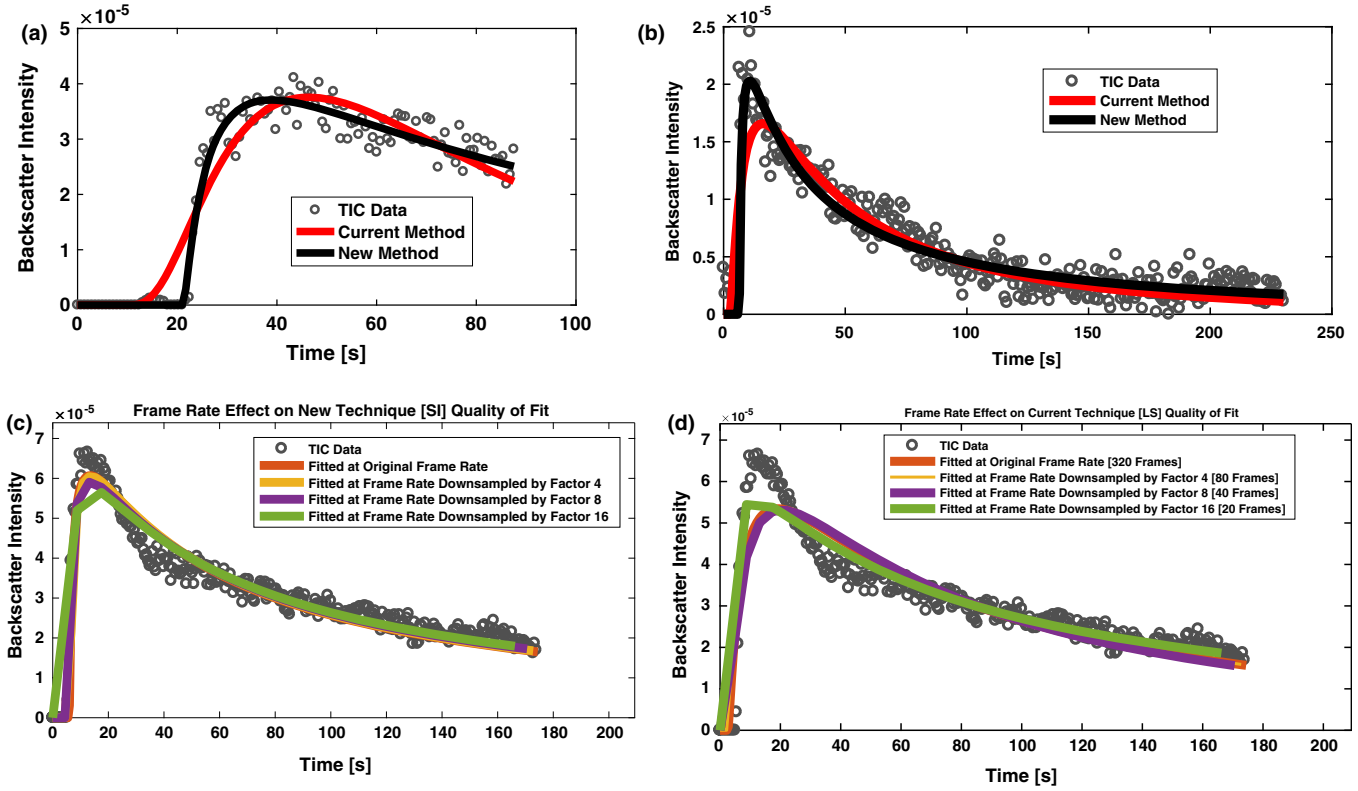

FIG. 3. Comparison between our proposed approach (*in black*) and the current approach (*in red*) to evaluate (a) the effect of offset time on the perfusion model using the lognormal function for typical bolus time–intensity curve (TIC) data from a mouse tumor. Gray circles represent the original TIC data. As can be seen in red, both the offset time (t_0) and time to peak are incorrect, resulting in a poorer fit, which happens because the wrong boundary conditions and model were selected. The quality fit using the new method is much closer to the expected perfusion parameters compared to the current method. (b) When the original TIC data are very noisy, the new method also performs much better compared to the current approach. Fitting to the lognormal tracer model using (c) our new method and (d) the current method with the original frame rate and various down-sampled frame rates. The lognormal tracer model was used to estimate perfusion parameters, and the estimated parameters using the new method are closer to the expected values for perfusion parameters for any given frame rate. Greater down-sampling is expected to degrade curve fitting performance, and the new method is much more robust to high levels of down-sampling. TIC data come from dynamic contrast-enhanced ultrasound images of a typical mouse tumor. [Color figure can be viewed at wileyonlinelibrary.com]

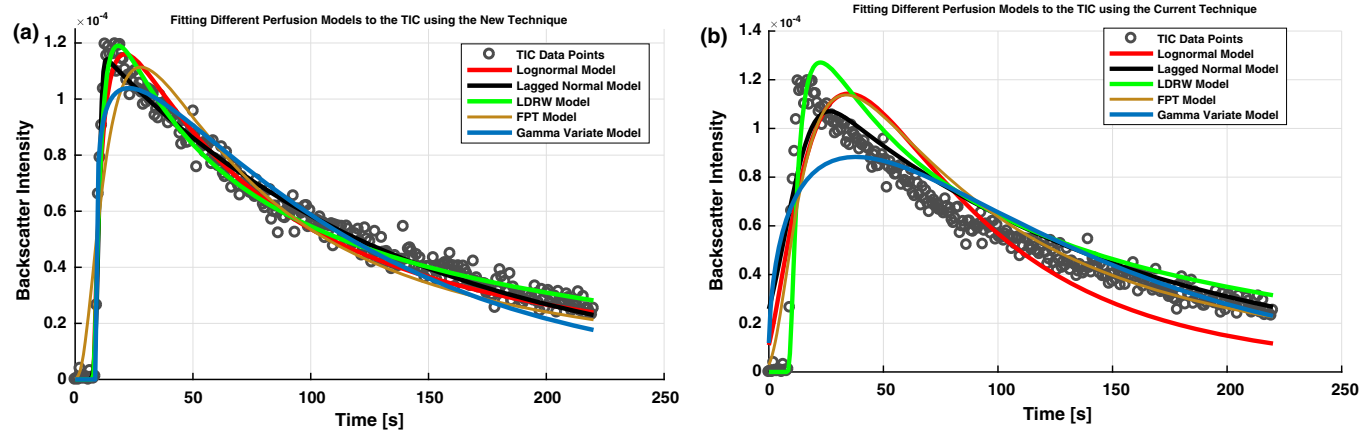

(c)

New (Proposed) Method:

Model	R^2	Spearman Correlation	NRMSE
Log Normal	0.9764	0.9264	0.3460
Lagged Normal	0.9779	0.9209	0.2824
LDRW	0.9788	0.9744	0.1602
FPT	0.9496	0.7728	0.5403
Gamma Variate	0.9728	0.8506	0.4150

Current (Existing) Method:

Model	R^2	Spearman Correlation	NRMSE
Log Normal	0.9318	0.8026	0.5506
Lagged Normal	0.9470	0.8497	0.4406
LDRW	0.9691	0.9290	0.4007
FPT	0.9567	0.8423	0.4538
Gamma Variate	0.9222	0.7362	0.5283

FIG. 4. Comparison of the performance of different perfusion models using (a) the multi-model framework showing the quality of fit for each perfusion model (new method) and (b) the least-squares method (current method). The raw time–intensity curve data are represented by gray circles. (c) Quantification of the aforementioned results by R^2, Spearman correlation, and normalized root-mean-squared error is provided. [Color figure can be viewed at wileyonlinelibrary.com]

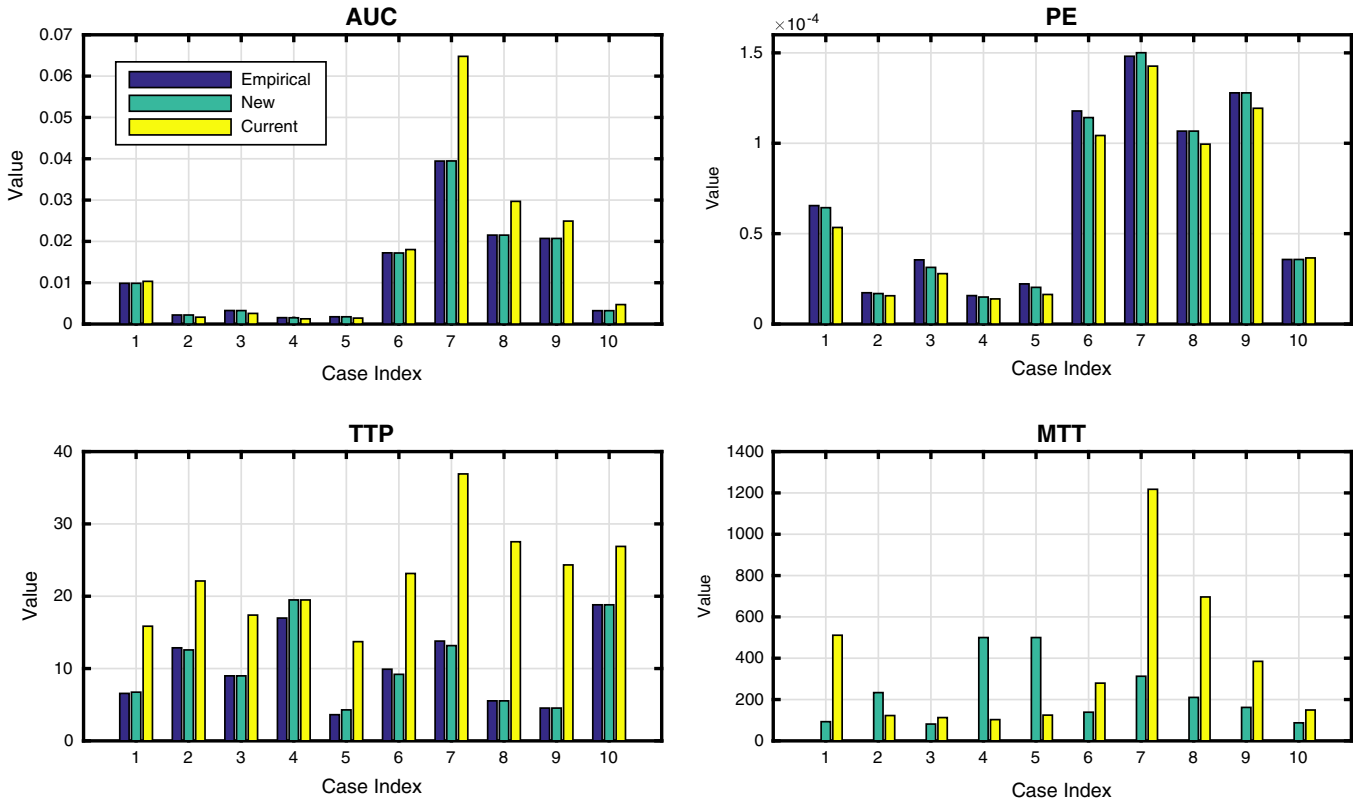

FIG. 5. Values for perfusion parameters using the current single model method (least-squares) in yellow color bars, performance of the new method (multi-model framework) in green bars, and the empirical values for perfusion parameters in dark blue. The new method was consistently closer to the empirical perfusion parameters. Perfusion parameters include area under the curve, peak enhancement, time to peak, and mean transit time (MTT). Please note that MTT could not be calculated empirically. Table II compares the goodness-of-fit by three different measures (coefficient of determination, Spearman correlation, normalized root-mean-squared error), also finding that the new method has the best performance. [Color figure can be viewed at wileyonlinelibrary.com]

TABLE II. Comparison of quality of fit between the current and new methods.

	R^2	Spearman	NRMSE
(A) New method			
Mean	0.95128	0.95995	0.19187
Median	0.97781	0.96886	0.17587
STD	0.044599	0.023023	0.057463
(B) Current method			
Mean	0.90128	0.90128	0.31272
Median	0.90657	0.90657	0.3087
STD	0.026475	0.026475	0.040992

Predicted perfusion parameters and quality of fit for (A) our proposed technique (multi-model framework using system identification) and (B) the current technique (least-squares optimization). Between the ten mouse cases, the new method on average has a higher coefficient of determination (R^2), higher Spearman correlation coefficient, and a lower normalized root-mean-square error compared to the current method. These quantified results are presented as a bar plot in Fig. 5.

5. DISCUSSION

We compared the performance of conventional single-model perfusion modeling using least-squares optimization and our proposed multi-model framework that analyzes different perfusion models, including lognormal, gamma variate, LDRW, FPT, and lagged normal. As shown in Fig. 5, we found that our proposed framework results in perfusion parameter estimation far closer to empirical data than the current approach. The accuracy of the current and proposed methods was investigated using both synthetic TIC data and real TICs from a preclinical mouse tumor model. It is less sensitive to issues affecting quality of fit to TIC data, such as frame rate, ROI size, noise, and rise time. For instance, a frame rate greater than 10 Hz is suggested for adequate visualization and recording of the wash-in patterns during hepatic lesion characterization.[12] We conclude that our proposed multi-model framework outperforms the existing technique, a single-model approach using least-squares curve fitting. Our proposed framework applies different perfusion models (lognormal, gamma variate, lagged normal, LDRW, and FPT) and returns perfusion parameters (t_0, AUC, TP, MTT, and PE) based on the perfusion model with the best fit. Thus, to ensure that the perfusion parameters are accurately estimated, a multi-model framework approach is essential. This approach will aid in the selection of the best application-specific perfusion model.

Previous studies have looked at individual perfusion models or modifications of them. For instance, a previous work examined the gamma-variate function specifically and modified it such that it accounted for the trapping of microbubbles within the vasculature, showing that this inclusion increased

classification performance.[36] One article showed that a model with an arterial input function, based on the kinetics of a feeding artery and an estimated time-delay parameter, could fit contrast kinetics similarly compared to the lognormal model.[37] Another study analyzed five perfusion models—Tofts, Extended Tofts, Two-compartment model, Tissue-Homogeneity, and Distributed Parameter—by performing a sensitivity analysis and identifiability analysis, compared parameter variance and model error on simulated curves, and generated parametric maps using CT data.[38] In comparison, our study provides a framework that can be applied to any tissue that automatically selects the best perfusion model and curve fitting algorithm, it was tested with model perturbations that simulate real-life ultrasound imaging considerations, and it was shown to provide better performance than the traditional method when applied to DCE-US data, evaluating against empirically derived ground truth data.

The benefit of this work is more precise estimation of perfusion parameters, which will be essential for the many applications of CEUS. For instance, tumor volume might not always change with treatment, but changes in perfusion parameters may confirm whether treatment is actually working. In addition, this is an organ-independent approach, which will not require the selection of a different perfusion model for different organs.[19] Moreover, this method is more robust, as it is much less sensitive to the initial selection of boundary conditions than is the current approach. With this hybrid approach to choose the most appropriate model, perfusion parameters can be measured more accurately. There are no widely accepted guidelines for the best perfusion model for each organ and animal model. However, this approach will provide the best model for each organ automatically, with no need for an expert to manually analyze the data. This will help in establishing an application-specific model for *in vivo* data.

There are a few limitations of this work that could be addressed in a future study. First of all, this work only analyzed one tumor type in mice. In future directions, we want to apply this algorithm to both other tumor types and human data and further optimize it based on these data. We would also like to use it for treatment effectiveness monitoring, a form of longitudinal analysis. This paper solely focused on untreated mice, and a paper focusing on treatment could analyze different time points or compare the relative importance of perfusion parameters vs lesion size. Finally, as this was predominantly a methods development paper, only a small sample of mice was analyzed ($n = 10$) to show some applicability of these models to real world data. Nevertheless, this study used animal data obtained under a controlled environment using standardized procedures[39], which is markedly different form data obtained from a clinical environment. However, it is important for a future applications paper to examine a substantially larger sample size.

6. CONCLUSIONS

We compared the current and our proposed techniques for perfusion parameter estimation and evaluated whether the latter technique can overcome common factors affecting the quality of fit to TIC data (rise time, frame rate, noise, and ROI size). We also performed an intersubject sensitivity analysis to check if the new technique is robust across subjects. Based on our results, the existing technique using least-squares curve fitting is much more sensitive to the aforementioned factors compared to our proposed technique. A robust multi-model framework for estimating perfusion parameters will reduce the amount of manual work required to tune the initial parameters and boundary conditions for curve fitting, saving a substantial amount of time. It will allow us to apply the proposed perfusion modeling framework to multiple datasets in an automated manner, greatly facilitating the analysis of diverse cases of perfusion data.

ACKNOWLEDGMENTS

The authors acknowledge the contributions of the late Dr. Jürgen Willmann, whose guidance was essential to this work. We also acknowledge Dr. Jianhua Zhou for conducting the original animal experiments used by this study. Hersh Sagreiya was supported by an RSNA Research Fellow Grant from the Radiological Society of North America, as well as with funding from the Stanford Cancer Imaging Training Program.

CONFLICTS OF INTEREST

The authors have no relevant conflicts of interest to disclose.

*Deceased January 8, 2018.
[a)]Author to whom correspondence should be addressed. Electronic mail: dlrubin@stanford.edu; Telephone: (650) 497-0440; Fax: 650-723-5795.

REFERENCES

1. Chung WS, Park MS, Shin SJ, et al. Response evaluation in patients with colorectal liver metastases: RECIST version 1.1 versus modified CT criteria. *AJR Am J Roentgenol*. 2012;199:809–815.
2. Anzidei M, Napoli A, Zaccagna F, et al. Liver metastases from colorectal cancer treated with conventional and antiangiogenetic chemotherapy: evaluation with liver computed tomography perfusion and magnetic resonance diffusion-weighted imaging. *J Comput Assist Tomogr*. 2011;35:690–696.
3. Meier R, Braren R, Kosanke Y, et al. Multimodality multiparametric imaging of early tumor response to a novel antiangiogenic therapy based on anticalins. *PLoS ONE*. 2014;9:e94972.
4. Lampaskis M, Averkiou M. Investigation of the relationship of nonlinear backscattered ultrasound intensity with microbubble concentration at low MI. *Ultrasound Med Biol*. 2010;36:306–312.
5. Strouthos C, Lampaskis M, Sboros V, McNeilly A, Averkiou M. Indicator dilution models for the quantification of microvascular blood flow with bolus administration of ultrasound contrast agents. *IEEE Trans Ultrason Ferroelectr Freq Control*. 2010;57:1296–1310.
6. El Kaffas A, Sigrist RMS, Fisher G, et al. Quantitative three-dimensional dynamic contrast-enhanced ultrasound imaging: first-in-human pilot study in patients with liver metastases. *Theranostics*. 2017;7:3745–3758.

7. Wasmeier GH, Zimmermann WH, Schineis N, et al. Real-time myocardial contrast echocardiography for assessing perfusion and function in healthy and infarcted wistar rats. *Ultrasound Med Biol*. 2008;34:47–55.
8. Thijssen JM, de Korte CL. Modeling ultrasound contrast measurement of blood flow and perfusion in biological tissue. *Ultrasound Med Biol*. 2005;31:279–285.
9. Zhou J, Zhang H, Wang H, et al. Early prediction of tumor response to bevacizumab treatment in murine colon cancer models using three-dimensional dynamic contrast-enhanced ultrasound imaging. *Angiogenesis*. 2017;20:547–555.
10. Wang H, Hristov D, Qin J, Tian L, Willmann JK. Three-dimensional dynamic contrast-enhanced us imaging for early antiangiogenic treatment assessment in a mouse colon cancer model. *Radiology*. 2015;277:424–434.
11. Szabo BK, Saracco A, Tanczos E, et al. Correlation of contrast-enhanced ultrasound kinetics with prognostic factors in invasive breast cancer. *Eur Radiol*. 2013;23:3228–3236.
12. Dietrich CF, Averkiou M, Nielsen MB, et al. How to perform contrast-enhanced ultrasound (CEUS). *Ultrasound Int Open*. 2018;4:E2–E15.
13. Sjöberg J, Zhang Q, Ljung L, et al. Nonlinear black-box modeling in system identification: a unified overview. *Automatica*. 1995;31:1691–1724.
14. Sedgewick R, Wayne KD. *Algorithms* (4th ed.) deluxe. ed. Boston, MA: Addison-Wesley; 2016.
15. Tarantola A, Valette B. Generalized nonlinear inverse problems solved using the least squares criterion. *Rev Geophys Space Phys*. 1982;20:219–232.
16. Harabis V, Kolar R, Mezl M, Jirik R. Comparison and evaluation of indicator dilution models for bolus of ultrasound contrast agents. *Physiol Meas*. 2013;34:151–162.
17. Biondi B, Almomin A. Tomographic full-waveform inversion (TFWI) by combining FWI and wave-equation migration velocity analysis. *Lead Edge*. 2013;32:1074–1080.
18. Symes WW. The seismic reflection inverse problem. *Inverse Prob*. 2009;25:123008.
19. Lampaskis M, Strouthos C, Averkiou M. Application of tracer dilution models for the quantification of perfusion with contrast enhanced ultrasound imaging. 14th European Symposium on Ultrasound Contrast Imaging; Rotterdam, The Netherlands. 2009.
20. Stow RW, Hetzel PS. An empirical formula for indicator-dilution curves as obtained in human beings. *J Appl Physiol*. 1954;7:161–167.
21. Koch AL. The logarithm in biology II. Distributions simulating the log-normal. *J Theor Biol*. 1969;23:251–268.
22. Thompson HK, Whalen RE, Starmer CF, Mcintosh HD. Indicator transit time considered as a gamma variate. *Circulation*. 1963;28:816.
23. Wise ME. Tracer dilution curves in cardiology and random walk and lognormal distributions. *Acta Physiol Pharm N*. 1966;14:175.
24. Mischi M, Jansen AHM, Korsten HHM. Identification of cardiovascular dilution systems by contrast ultrasound. *Ultrasound Med Biol*. 2007;33:439–451.
25. Davis GC, Kutner MH. Lagged normal family of probability density functions applied to indicator-dilution curves. *Biometrics*. 1976;32:669–675.
26. Heiberger RM, Becker RA. Design of an S-function for robust regression using iteratively reweighted least-squares. *Comput Sci Stat*. 1992;24:112–116.
27. Oleary DP. Robust regression computation using iteratively reweighted least-squares. *Siam J Matrix Anal A*. 1990;11:466–480.
28. West BT, Galecki AT. An overview of current software procedures for fitting linear mixed models. *Am Stat*. 2011;65:274–282.
29. Seber GAF. Nonlinear regression models. Springer Ser Stat. 2015:117–128.
30. Dumouchel W, O'Brien F. Integrating a robust option into a multiple regression computing environment. In: *Computing and Graphics in Statistics*. New York, NY: Springer-Verlag New York, Inc.; 1991:41–48.
31. Natrella M. *NIST/SEMATECH e-handbook of statistical methods.* NIST/SEMATECH; 2010.
32. Payen T, Coron A, Lamuraglia M, et al. Echo-power estimation from log-compressed video data in dynamic contrast-enhanced ultrasound imaging. *Ultrasound Med Biol*. 2013;39:1826–1837.
33. Moré J. The levenberg-marquardt algorithm: implementation and theory. In: Watson GA, ed. *Numerical Analysis*. Berlin, Germany: Springer-Verlag; 1978:105–116.
34. Gupta M, Taneja H, Chand L. Performance enhancement and analysis of filters in ultrasound image denoising. Paper presented at: International Conference on Computational Intelligence and Data Science. 2018.
35. Jacobs M, Benovoy M, Chang LC, Arai AE, Hsu LY. Evaluation of an automated method for arterial input function detection for first-pass myocardial perfusion cardiovascular magnetic resonance. *J Cardiovasc Magn Reson*. 2016;18:17.
36. Rizzo G, Tonietto M, Castellaro M, et al. Bayesian quantification of contrast-enhanced ultrasound images with adaptive inclusion of an irreversible component. *IEEE Trans Med Imaging*. 2017;36:1027–1036.
37. Doury M, Dizeux A, de Cesare A, et al. Quantification of tumor perfusion using dynamic contrast-enhanced ultrasound: impact of mathematical modeling. *Phys Med Biol*. 2017;62:1113–1125.
38. Romain B, Rouet L, Ohayon D, Lucidarme O, d'Alche-Buc F, Letort V. Parameter estimation of perfusion models in dynamic contrast-enhanced imaging: a unified framework for model comparison. *Med Image Anal*. 2017;35:360–374.
39. Hyvelin JM, Tardy I, Arbogast C, et al. Use of ultrasound contrast agent microbubbles in preclinical research: recommendations for small animal imaging. *Invest Radiol*. 2013;48:570–583.

SUPPORTING INFORMATION

Additional supporting information may be found online in the Supporting Information section at the end of the article.

Appendix S1: Mixed-Effects Models and Nonlinear Regression Based Models.
Appendix S2: Animal data acquisition.